MICROTEXTURE INVESTIGATION OF ORIENTATION GRADIENTS AND GRAIN SUBDIVISION IN ROLLED COARSE-GRAINED NIOBIUM

H.R.Z. Sandim

Department of Materials Engineering
FAENQUIL, P.O. Box 116
12600-000 Lorena
Brazil

D. Raabe

Max-Planck-Institut für Eisenforschung
Max-Planck-Str. 1
40237 Düsseldorf
Germany

Keywords*: niobium, cold rolling, grain subdivision, EBSD, microtexture, orientation gradients*

Report abstract

Orientation effects concerning grain subdivision and further annealing behavior of three neighboring grains were observed in 80% cold-rolled coarse-grained niobium. The present study which was conducted as a cooperation on the basis of DAAD and CAPES funding attempts to clarify the microstructural evolution of deformed niobium and the differences in terms of stored energy (boundary distribution) using high-resolution electron backscattering diffraction (FE-EBSD).

Acknowledgments

Authors acknowledge CAPES-DAAD for providing support for this work. The kind assistance of Mrs. Katja Angenendt (MPI, Düsseldorf, Germany) in FE-SEM-EBSD is also acknowledged. HRZS is CNPq Fellow under Grant No. 300.158/2002-5. Thanks are also due to MSc. J.F.C. Lins (DEMAR, FAENQUIL, Brazil) for supplying the Nb specimens.

1. Introduction

The microstructure of high-purity niobium ingots processed by electron beam melting mostly consists of a few columnar grains with sizes in the centimeter-range. The plastic deformation of coarse-grained materials usually leads to a very inhomogeneous microstructure [1,2]. Orientation effects were already reported in literature concerning grain subdivision and further annealing behavior of coarse-grained refractory metals like niobium and tantalum [3-6]. In both cases, the substructure was found to vary significantly from one grain to another. The knowledge of the magnitude of the misorientation angles formed during grain fragmentation is essential to understanding nucleation and further recrystallization behavior in coarse-grained niobium.

High resolution electron backscattering diffraction (EBSD) coupled to a field emission gun scanning electron microscope (FE-SEM) has proven to be a powerful analytical tool and has many advantages on conventional SEM including higher mapping speed, improved spatial resolution (down to the 20 nm-range), and reduced chromatic aberration [7,8]. In addition, large areas can be mapped compared to TEM enabling an enhanced statistical basis. On the other hand, its limited angular resolution does not allow distinguishing cells or subgrains with small misorientations usually below 2°.

The present paper presents the main results concerning grain subdivision aspects in three neighboring grains in 80% cold-rolled niobium using the FE-EBSD technique. The results concerning misorientation distributions indicate strong orientation effects in the cold-rolled material.

2. Experimental

A high-purity coarse-grained niobium ingot was obtained by means of multiple electron beam melting (EBM). Interstitial (O<50, N<5, wt-ppm) and metallic (W<55, Fe<45, Al<30 and Si<50, wt-ppm) impurity contents are in agreement with ASTM-B-391-99 (reactor-grade purity). In the initial state the ingot consisted of columnar grains with grain boundaries lying nearly parallel to the rolling direction (RD). These grains are 10 to 30-mm wide and 40 to 200-mm long. A thick slab (50 mm in thickness x 140 mm wide x 300 mm long) was cut from the center of this ingot and then cold rolled to a total reduction in thickness of 80% (true strain $\varepsilon = 1.6$). Three consecutive grains were sampled in the longitudinal section of the rolled plate. Metallographic preparation of sections was carried out using conventional techniques including intermediary chemical polishing to remove surface deformation. The microstructures of both cold-rolled and annealed specimens were observed in detail in a JEOL JSM-6500F field emission scanning electron microscope (FE-SEM) operating at 15 kV. The EBSD scans were carried out in areas of about 120 x 50 μm^2 in the longitudinal plane (RD-ND plane, where RD is the rolling direction and ND is the normal direction). EBSD sampling points were performed in every 0.1 μm (corresponding to the map step size). Microtexture evaluation was determined by means of automated acquisition and further indexing of Kikuchi patterns after suitable image processing in a TSL system interfaced to the FE-SEM. Mapping speed varied from 10 to 15 patterns per second. Pole figures and misorientation (ψ) distributions were determined for each mapped region. Two adjacent areas of each grain in the vicinity of the prior grain boundary were scanned to allow comparison between grains. From now on, these boundaries are named A-B and B-C.

3. Results

The microstructure of 80% cold-rolled niobium displays elongated grains with grain boundaries aligned nearly parallel to the rolling direction. Assuming an initial grain size in normal direction of about 10 mm prior to rolling, one expects that the original grains have thinned to about 2 mm thickness.

The substructure developed after cold rolling differs markedly from one grain to another. Fig. 1a shows these three grains in close detail in SEM. Channeling contrast does not resolve all details of the microstructure; however, this technique allows identifying regions of extension above about 1 μm with misorientations relative to their neighborhood by more than 1°. The Kikuchi patterns obtained during FE-EBSD measurements were very sharp easing further computer-assisted orientation indexing. Large mappings of about 60 x 50 μm^2 were performed in each grain. Taking into account the predicted grain size for this material after 80% cold rolling, the results shown in this paper represent the behavior of these grains at their respective grain boundary regions.

Grains A and C developed lamellar structures nearly parallel to RD. Grain B, on the other hand, developed a coarser structure. Bands of localized shear making about 45° with respect to the rolling direction are present subdividing the microstructure of grain B. Grain B rotates slightly from one boundary to another. The orientation spread of grain B also increases when boundary B-C approaches, as shown in the corresponding poles figures displayed in Fig. 1. A fairly organized subgrain structure is found in grain B. They are very diffuse at OIM and can only be distinguished by shading among different regions corresponding to low local lattice misorientations. As a general comment, the orientation spread around TD is more pronounced that around RD for all grains.

The differences in terms of grain subdivision and developed misorientations can be quantified when data from FE-EBSD are analyzed. Orientation maps from EBSD data are shown in Fig. 2. They show relevant orientation effects concerning grain subdivision of the three grains. The initial orientation of grain B was probably very close to Goss, {011} <001>. Orientations close to Goss are known to be very unstable and tend to split about the transverse direction (TD) under plane strain loading as will be discussed in the next section.

The transition from one grain to another can be easily distinguished in grain boundary A-B. In a contrasting manner, boundary B-C appears displaying a narrow transition zone of about 20 μm where the original grain boundary cannot be easily recognized, at least at first sight. It is worth mentioning that coarse in-grain orientation gradients are present in grain C (see right part of Fig. 2b). Grain A, on the other hand, shows narrow bands, 1-2 μm spaced, and lying parallel to RD. The misorientation across these bands is typically above 40°.

Fig. 3 displays grain boundary misorientation distribution histograms for grains A, B, and C taking into account only boundaries with $\psi > 2°$. The distributions are based on data taken from equal-size areas cropped from each grain. The results from boundary A-B indicate that grain A has subdivided in a wide range of misorientations with many boundaries having high angle character ($\psi > 15°$). The spacing among high-angle boundaries in grain A was found to be about 2.1 μm using the linear intercept method. On the other hand, the cumulative distribution shows that low angle boundaries are predominant in grain B ($\psi < 10°$). A few boundaries with misorientations above 15° are also present close to grain boundary A-B. Boundary B-C displays a similar feature. The distribution of misorientation angles in grain B changes when approaching boundary B-C. A slightly higher fraction of high-angle boundaries is present compared to that observed at boundary A-B. Despite of

its coarser structure, grain C contains more high-angle boundaries than grain A, at least in the grain boundary region. The spacing between high-angle boundaries, in this case, was smaller, namely, close to 1.6 μm.

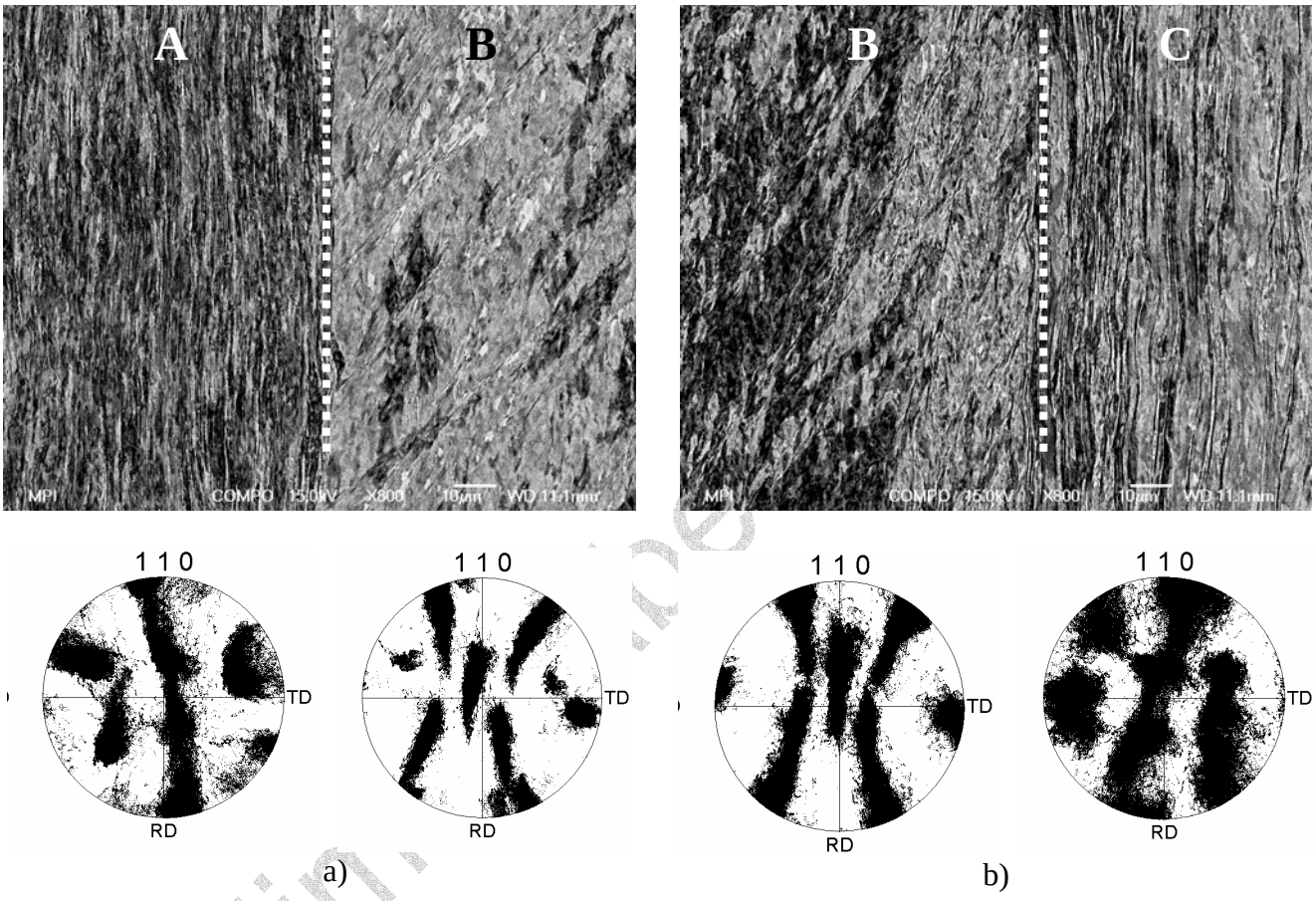

Figure 1 - Longitudinal sections of grains A, B, and C showing their microstructures and corresponding pole figures in 80% cold-rolled niobium (FE-SEM, backscattered electrons): a) boundary A-B; b) boundary B-C. RD is the rolling direction; TD is the transverse direction. Grain boundary (dashed line) lies nearly in the center of each micrograph. RD is parallel to vertical. ND is parallel to the horizontal.

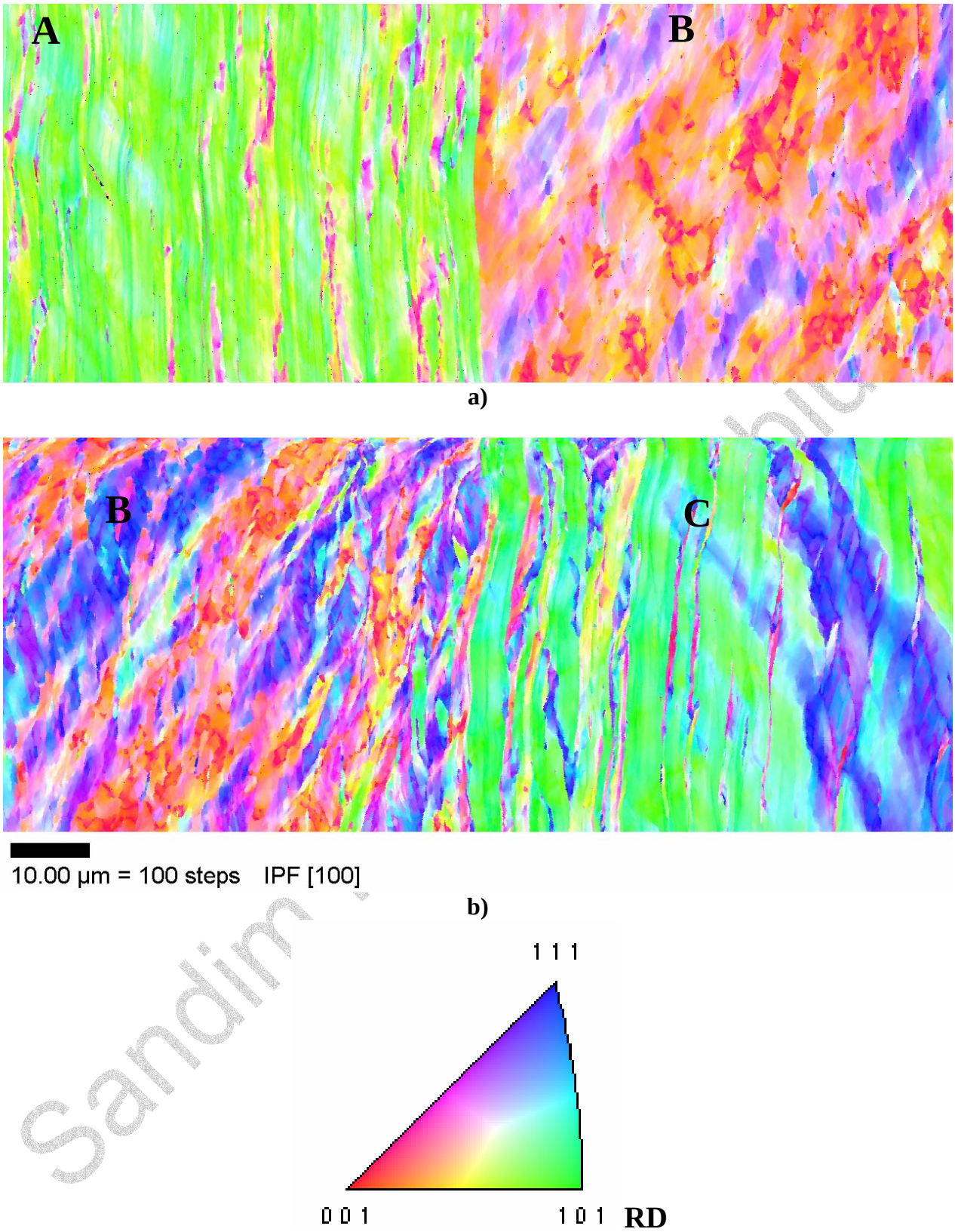

Figure 2 – Electron backscatter diffraction maps showing details of the grain boundary region of: a) grains A and B; b) grains B and C. Color coded map referred to RD is shown at right side. RD is parallel to vertical. ND is parallel to the horizontal.

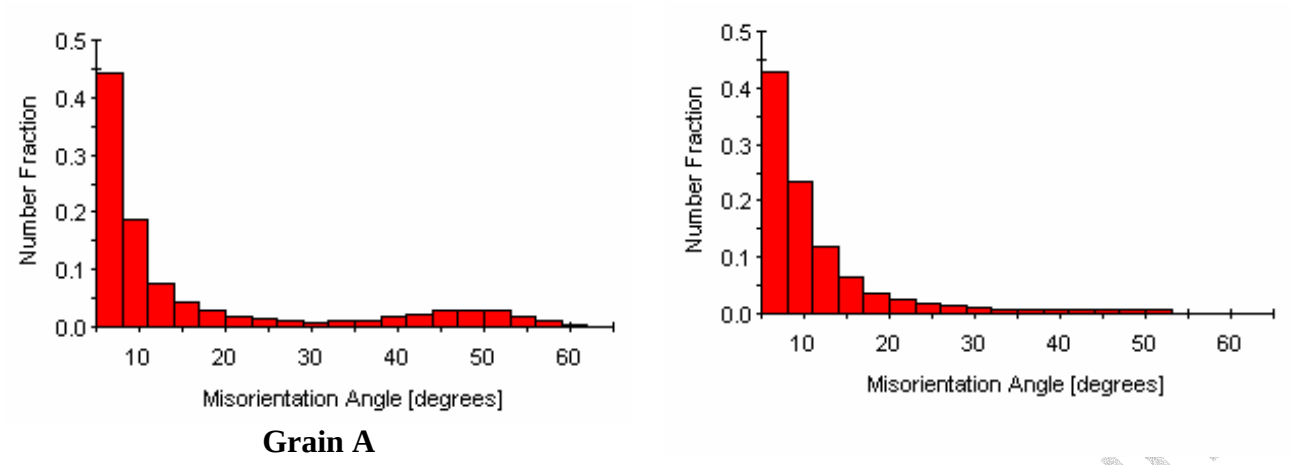

a) Boundary A-B

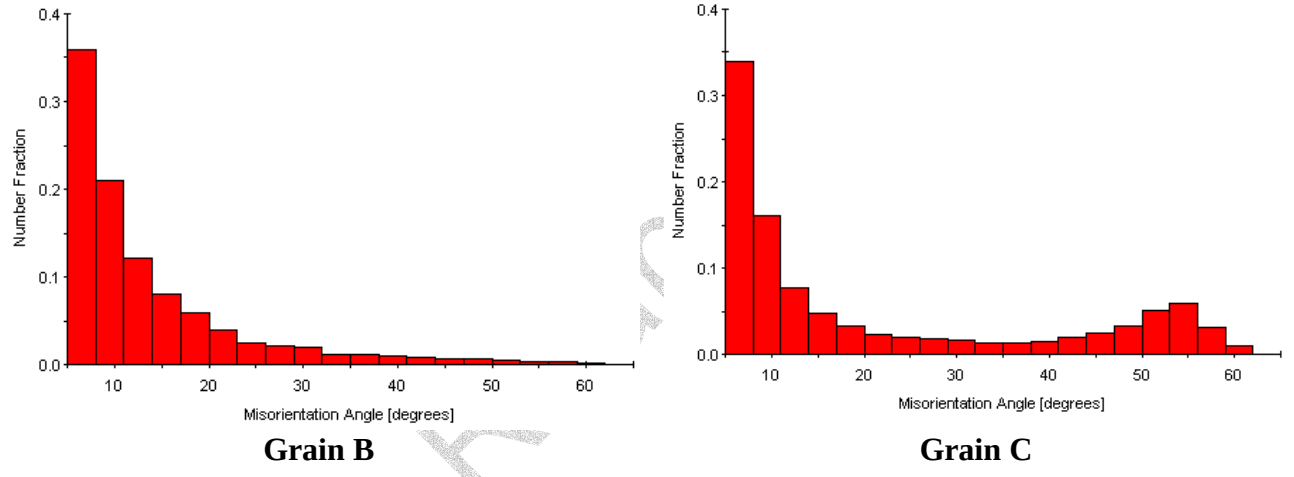

b) Boundary B-C

Figure 3 – Boundary misorientation distribution determined in transverse section of grains A, B, and C from FE-EBSD measurements in boundaries counting only misorientation above $\psi > 2°$: a) A-B; b) B-C.

In consequence of the pronounced differences observed in the deformed state, the three grains behaved quite inhomogeneously during annealing. Strong local differences in the rate of static recrystallization were observed, similar as in recrystallizing large iron grains [9]. Fig. 4 shows the microstructure of a region comprising grains A, B, and C after annealing at 900°C for 1 h. Recrystallization was incomplete in grain A. The new grains with elongated morphology have nucleated at highly misoriented bands as shown in Fig. 1a. Grain B, on the other hand, displayed a higher recrystallized volume fraction (X_{rx} > 90%). The recrystallized grain size in this case was

about 90 μm. Full recrystallization was found to occur in former grain C. A finer equiaxed structure having a grain size close to 30 μm is clearly seen at the left side of Fig. 4.

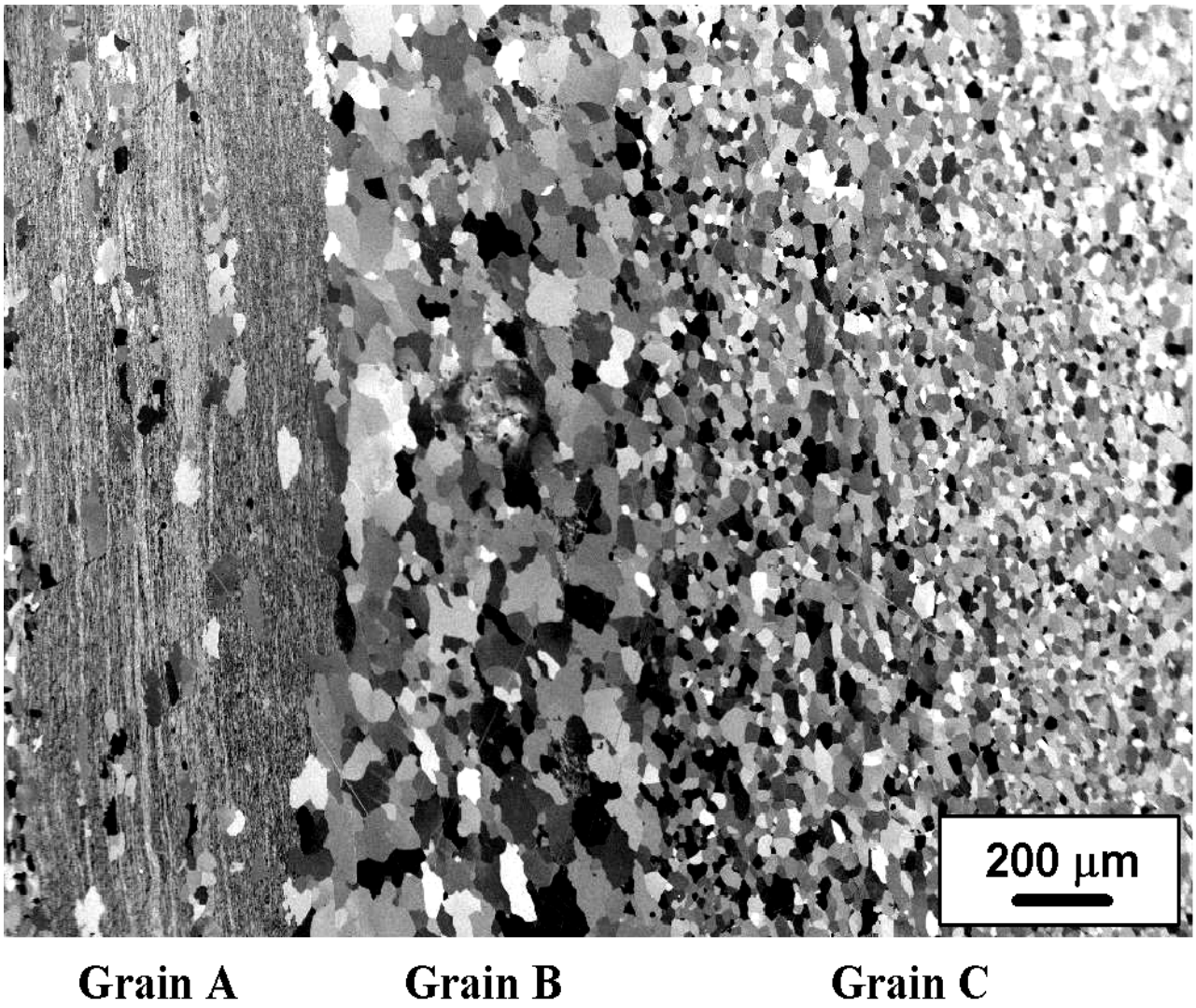

Figure 4 - Longitudinal sections of former grains A, B, and C showing their respective microstructures after annealing at 900°C for 1 h (FE-SEM, backscattered electrons). RD is parallel to vertical. ND is parallel to the horizontal. Position of former grains A, B, and C is indicated.

4. Preliminary Evaluation of the Experimental Results

The in-grain heterogeneity in terms of the deformation structure and the orientation dependence of these effects in coarse-grained niobium are evident. The microstructural evolution of niobium during cold rolling can be described in terms of grain subdivision by generation of geometrically necessary boundaries (GNB) to accommodate the increasing lattice misorientations [2,10]. In a previous paper, the heterogeneity of deformation microstructure in coarse-grained tantalum deformed by cold swaging was reported [4]. Distinct substructures were found to vary from one grain to another indicating strong orientation effects. The presence of lamellar structures in grains A and C at large strains are in agreement with those described by the grain subdivision model developed for medium-to-high stacking fault energy (SFE) metals [10,11]. At large strains ($\varepsilon \approx 1$), most of these dislocation boundaries tend to reorient into a lamellar structure having a wide range of misorientations, many of them with high angle character [11,12]. This model was based on extensive TEM investigated of thin foils of deformed metals with grain sizes normally below 300 μm, at least one order of magnitude smaller than the grain size found in EBM-Nb.

The tendency of grain subdivision into set of lamellae of strongly different orientations is distinctly orientation-dependent [13]. The results shown in this investigation confirm that the deformation behavior of each grain depends clearly on their initial orientation. In-grain orientation gradients are observed in all three grains but both, the orientational spread and the lateral arrangement of the differently oriented lamellae dependes on the particular orientation under inspection.

One important result which has not been observed before in experiment in this context is the orientation spread ocurring in grain B which has a main orientation close to the Goss component (see the two pole figures shown in Fig. 1). The data in the {110} pole figure reveal a strong orientation spread about the Goss which is characterized by two pronounced symmetric orientation branches which are related to each other by a rotation about the transverse direction. In a recent theoretical treatment [13] orientations close to the Goss were indeed predicted to undergo such an orientation split under plane strain loading. The predictions were made using both, homogenization theory and a crystal plasticity finite element approach. The theoretical treatment for the prediction of in-grain orientation gradients was essentially built on the divergence of the re-orientation fields of the respective texture component.

Fig. 5 shows a in-grain texture in a deformed Goss crystal of a body centered cubic material under plane strain loading in the form of a {111} pole figure. The open squares shows the initial orientation (which was the same at all integration points) and the black dots show the orientations after deformation. The deformed grain is characterized using a the accumulated misorientations in a gray scale coding (light values indicate large misorientations). The crystal plasticity finite element simulations were conducted by using 48 slip systems to a thickness reduction of 50%. The data reveal very good agreement to the two experimental pole figures given for grain B in Fig. 1 (note that the pole figures in Fig. 1 are {110} instead of {111} projections).

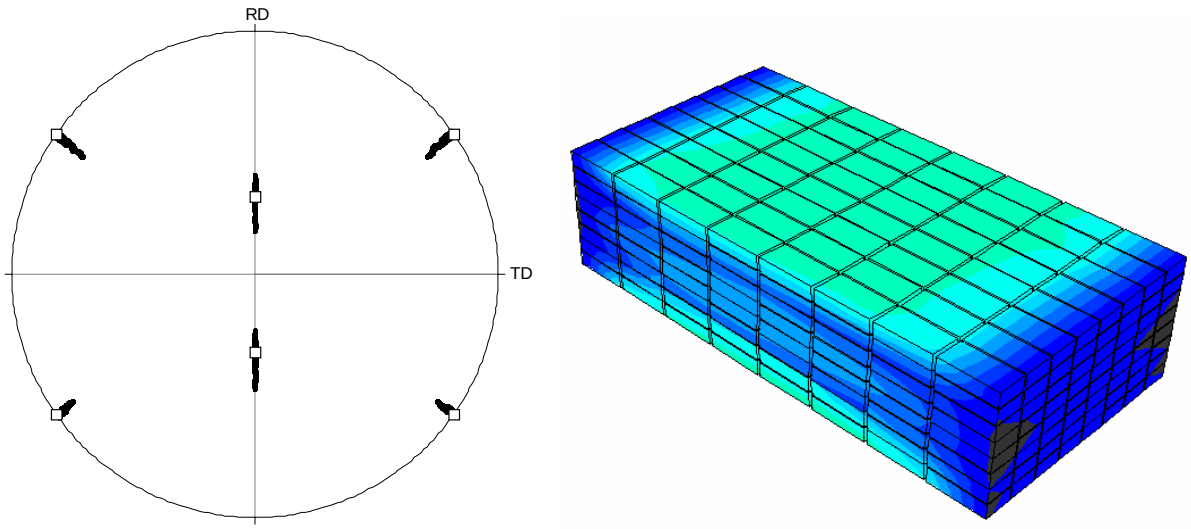

Figure 5 - In-grain texture in a deformed Goss crystal of a body centered cubic material under plane strain loading, {111} pole figure, 48 slip systems, thickness reduction of 50%, color scale coding indicates accumulated misorientations.

The recrystallization behavior of this material depends on the nature of these orientation gradients developed within individual grains. It is well known that nucleation and growth of new grains in deformed metals is driven by the stored energy within each grain. The stored energy depends on the nature and misorientation range of the deformation induced dislocation boundaries [14]. In special, deformation-induced boundaries with large curvatures like most of the lamellar boundaries (LBs) provide potential nucleation sites for recrystallization. In that sense, the FE-EBSD technique combined to the mappng of the channeling contrast at SEM provides a powerful tool to investigate the deformed state of severly strained materials. Effective spatial resolutions in the nm-range are a clear advantage of this technique compared to conventional SEM, especially where lamellar boundaries are spaced in the submicron-range. Besides, this technique gains more relevance when large maps are required, especially when the grain size in the deformed state is still in the mm-range as in the present case.

In-grain orientation gradients may also have their origin due to extrinsic factors [13]. Depending on the orientation of neighboring grains, the nature of the substructure close to the grain boundaries might be affected. This is in agreement with the observation concerning boundary misorientations in grain B. Depending on its neighborhood (grain A or grain C), changes in the misorientation distribution are expected to occur, especially at the vicinity of the grain boundaries.

Annealing at low homologous temperatures is a useful method to investigate changes in recovery and recrystallization kinetics in coarse-grained materials. Important aspects like recrystallized grain size, recrystallized volume fraction, and preferential nucleation sites (grain boundaries and/or deformation heterogeneities) can be investigated in detail by means of such a procedure. The results shown in this paper confirm the strong orientation effects on recrystallization in oligocrystalline niobium. The microstructure in the annealed state consists of layers displaying partial and full-recrystallized regions with large local variations in texture and grain size. Recrystallization in

former grain A was only partial and the nucleation of the new grains can be associated to the 40°-misoriented bands lying parallel to RD. The typical misorientation found in regions far from these bands was about 10° or even smaller. The finer grain size found in former grain C has to do with the higher fraction of high-angle boundaries in the deformed state, especially those above 45°. The former Goss-oriented grain (grain B) displayed an intermediary behavior compared to grains A and C. Its coarser grain structure in the annealed state can be explained by the presence of a lesser number of potential nucleation sizes but, contrasting with grain A, an advantage in terms of growth is evident.

5. Preliminary Project Conclusions

The results shown in the present progress report confirm the strong heterogeneity and the orientation dependence of both, deformation and annealing processes in coarse-grained niobium. The microstructure of 80% cold-rolled niobium reveals noticeable differences in terms of grain subdivision. Channeling contrast at SEM combined with orientation mapping provided by high-resolution field emission electron backscattering diffraction (FE-EBSD) measurements were used to characterize the microstructure. Boundary misorientation distributions were determined for three distinct grains indicating noticeable differences in terms of the stored energy. In consequence, recovery and recrystallization kinetics were found to vary significantly from one grain to another giving rise to an inhomogeneous structure.

References

[1] Hansen N, Metall. Trans. **16A** (1985) 2167-2190.

[2] Hansen N, Mater. Sci. Technol., **6** (1990) 1039-1047.

[3] Sandim HRZ, Lins JFC, Pinto AL, Padilha AF, Mater. Sci. Eng. **A-354** (2003) 217-228.

[4] Sandim HRZ, McQueen HJ, Blum W, Scripta mater., **42** (1999) 151-155.

[5] Raabe D, Lücke K, Gottstein G: Journal de Physique IV, colloque C7, supplément au Journal de Physique III **3** (1993) 523–526.

[6] Raabe D, Schlenkert G, Weisshaupt H, Lücke K: Mater. Sc. Technol. **10** (1994) 229–305.

[7] Mishin OV, Huang X, Bowen JR, Juul Jensen D, in: AR Dinesen, M Eldrup, D Juul Jensen, S Linderoth, TB Pedersen, NH Pryds, A Schrøder Pedersen, JA Wert (Eds.), Proceedings of the 22nd Risø International Symposium on Materials Science, Risø National Laboratory, Roskilde, Denmark, 2001, p.335.

[8] Isabell TC, Dravid VP, Ultramicroscopy 1997;67:59.

[9] Raabe D, Steel Research 66 (1995) 222–229.

[10] Bay B, Hansen N, Kuhlmann-Wilsdorf D, Mater. Sci. Eng., A-158 (1992) 139-146.

[11] Hughes DA, Hansen N, Metall. Trans., **24A** (1993) 2021.

[12] Hughes DA, Hansen N, Acta mater., **45** (1997) 3871.

[13] Raabe D, Zhao Z, Park S.-J., Roters, F, Acta Mater. **50** (2002) 421-440.

[14] Doherty, RD *et al*., Mat. Sci. Eng., **A238** (1997) 219-274.